

## Admittance estimates of mean crustal thickness and density at the Martian hemispheric dichotomy

Francis Nimmo

Department of Geological Sciences, University College London, London, UK

Received 14 March 2001; revised 23 April 2002; accepted 7 June 2002; published 30 November 2002.

[1] Admittance estimates from line-of-sight (LOS) acceleration profiles of the Mars Global Surveyor spacecraft are used to constrain the mean crustal thickness and surface density centered on the hemispheric dichotomy, from 110°E to 220°E, 40°S to 20°N. Models with uniform crustal properties predict lower than expected bulk crustal densities. Two-layer models with loading only at the surface and the Moho produce satisfactory fits to the data. The best fit surface density, crustal thickness  $t_c$ , and elastic thickness  $T_e$  are 2.5 Mg m<sup>-3</sup>, 27 km, and 61 km, respectively. Higher elastic thicknesses require lower crustal thicknesses, and vice versa. The best fit ratio of Moho to surface loading  $F$  is close to 1. Models with no bottom loading ( $F = 0$ ) provide a poor fit to the data; underestimates in  $F$  result in underestimates of both  $t_c$  and  $T_e$ . The surface density is lower than that measured from Martian meteorites and by admittance analyses of young volcanoes but is well constrained by the short-wavelength admittance values. For misfits up to 1.5 times the minimum value and a fixed surface density of 2.5 Mg m<sup>-3</sup>, the ranges of  $t_c$ ,  $T_e$ , and  $F$  are 1–75 km, 37–89 km, and 0.4–2.6, respectively. The apparently compensated nature of the large impact basins has been used to infer a lower bound on southern hemisphere crustal thickness of 45 km. If this estimate is correct, the likely mean crustal thickness in the area considered is  $55 \pm 20$  km. **INDEX TERMS:** 5417 Planetology: Solid Surface Planets: Gravitational fields (1227); 6225 Planetology: Solar System Objects: Mars; 8159 Tectonophysics: Evolution of the Earth: Rheology—crust and lithosphere; 8164 Tectonophysics: Evolution of the Earth: Stresses—crust and lithosphere; **KEYWORDS:** Loading, gravity, flexure, compensation, Mars Global Surveyor

**Citation:** Nimmo, F., Admittance estimates of mean crustal thickness and density at the Martian hemispheric dichotomy, *J. Geophys. Res.*, 107(E11), 5117, doi:10.1029/2000JE001488, 2002.

### 1. Introduction

[2] An obvious topographic feature on Mars is the hemispheric dichotomy, a difference in elevation of 2–4 km between the old (~4Gyr) southern highlands and the superficially younger northern lowlands [Smith *et al.*, 1999a]. Both the nature and the origin of the dichotomy remain uncertain [Esposito *et al.*, 1992]. This paper will place bounds on the mean crustal thickness, density and rigidity of an area centered on the dichotomy using line-of-sight (LOS) acceleration data. The results are compared with those of other authors using this technique [McKenzie *et al.*, 2002], and similar techniques using spherical harmonic representations of the gravity derived from the LOS data [McGovern *et al.*, 2002; Turcotte *et al.*, 2002; Zuber *et al.*, 2000].

[3] Spherical harmonic gravity data show small (~50 mGal) anomalies over the dichotomy, suggesting that it is approximately isostatically compensated [Smith *et al.*, 1999b]. Both Zuber *et al.* [2000] and Nimmo and Stevenson [2001] argue that the mean crustal thickness is unlikely to exceed 100 km, based on the fact that the dichotomy topography does not appear to have relaxed over 4 Ga.

Zuber *et al.* [2000] also find that  $T_e$  is generally <20 km for the southern highlands, but about 75 km for Elysium Mons (30°N, 150°E).

[4] As will be argued below, although the data may be fit by a single-layered crust of uniform density, the results are at odds with expectations of the nature of the Martian crust. Most of the results are therefore interpreted in terms of a two-layer crust, in which the near-surface is less dense than the underlying material. Because of the extra uncertainty introduced by the additional variables required by a two-layer model, considerable space is devoted to quantifying the likely errors in the results.

[5] Section 2 will discuss the theory of the admittance technique, and the use of a two-layer crustal model. Section 3 will discuss the implementation of the LOS admittance approach, and section 4 will present the results for the area of interest. The uncertainties in the results, and their implications, will be discussed in section 5.

### 2. Theory

[6] The admittance technique uses gravity and topography observations to infer the lithospheric elastic thickness  $T_e$ . One definition of the admittance estimate  $Z(k)$  is given by McKenzie and Fairhead [1997]

$$Z(k) = \frac{\langle \bar{g}\bar{t}^* \rangle}{\langle \bar{t}^* \rangle} \quad (1)$$

where  $k$  is the wave number ( $=2\pi/\lambda$ ),  $\bar{g}$  and  $\bar{t}$  are the Fourier transforms of the free-air gravity and topography, an asterisk denotes the complex conjugate and angle brackets denote the average value over a wave number band centered on  $k$ .

[7] The theoretical expressions for the admittance of an elastic plate [McKenzie, 1994] show that at long wavelengths the support is isostatic and thus  $Z \sim 0$ . At sufficiently short wavelengths the plate is not deformed by the load and thus

$$Z = 2\pi\rho_u G \quad (2)$$

where  $G$  is the gravitational constant and  $\rho_u$  is the density of the surface load. The short wavelength admittance may thus be used to determine the density independent of  $T_e$ . At intermediate wavelengths  $Z$  increases with  $k$ ; admittance estimates (equation 1) from planetary data can be fit by the theoretical expression to derive a value for  $T_e$ . There is generally a tradeoff between  $T_e$ ,  $\rho_u$  and the crustal thickness  $t_c$  in fitting a given profile [Barnett et al., 2000].

[8] It is generally assumed that the subsurface of a planet may be described as a layer of mean thickness  $t_c$  and constant density  $\rho_c$  overlying a half-space of higher density. Usually, this layer of higher density is assumed to represent the mantle and  $t_c$  thus represents the crustal thickness. However, on planets which have been heavily cratered (such as the Moon) the density of the crust may increase with depth as the amount of fracturing decreases [Simmons et al., 1973]. The fractured regolith on Mars has been estimated to be a few km thick [Clifford, 1993].

[9] Recently, the equations for the admittance of a two-layer crust have been derived by McKenzie [2002]. The crust consists of a top layer of thickness  $t_u$  and density  $\rho_u$  underlain by a layer of density  $\rho_l$ . The total thickness of the crust is  $t_c$ , the density of the fluid overlying the crust is  $\rho_w$  and that of the underlying mantle material is  $\rho_m$ . Here it will be assumed that the upper-lower crustal interface is initially flat. The interface will, however, be deformed by loads at the surface or at the Moho. If the fraction of surface and Moho loading are  $F_1$  and  $F_2$ , respectively, where  $F_1 + F_2 = 1$ , then the ratio of bottom to top loading  $F$  is given by

$$F = F_2/F_1. \quad (3)$$

[10] Both kinds of loading are assumed to produce surface topography. There may also be internal loads which produce a gravity signature but no topography; these will be referred to as incoherent loads [McKenzie, 2002] and have no effect on the value the admittance estimates, although they do increase the uncertainty. The relative importance of coherent and incoherent loads may be assessed by calculating the coherence between gravity and topography.

[11] Using the expressions of McKenzie [2002], the admittance  $Z$  is given by

$$Z = \frac{\sum_i F_i^2 Y_i^2 Z_i}{\sum_i F_i^2 Y_i^2} \quad (4)$$

where

$$Z_1 = -[(\rho_l - \rho_u) \exp(-kt_u) + (\rho_m - \rho_l) \exp(-kt_c)] / [(Dk^4/g) + \rho_m - \rho_u] \quad (5)$$

$$Z_2 = \left( \frac{\rho_l - \rho_u}{\rho_u - \rho_w} \right) \exp(-kt_u) - \left( \frac{1}{\rho_u - \rho_w} \right) [(Dk^4/g) + \rho_l - \rho_w] \exp(-kt_c) \quad (6)$$

$$Y_1 = \left( \frac{1}{\rho_u - \rho_w} \right) \frac{(Dk^4/g) + \rho_m - \rho_u}{(Dk^4/g) + \rho_m - \rho_w} \quad (7)$$

$$Y_2 = -1 / [(Dk^4/g) + \rho_m - \rho_w] \quad (8)$$

where  $k$  is the wave number,  $g$  is the acceleration due to gravity and  $D$  is the flexural rigidity, which is related to the elastic thickness  $T_e$  by

$$D = \frac{ET_e^3}{12(1 - \sigma^2)}. \quad (9)$$

Here  $E$  is the Young's modulus and  $\sigma$  is Poisson's ratio.

### 3. Method

[12] Equation (1) shows the relationship between admittance and gravity. Planetary gravity fields are generally expressed as spherical harmonic coefficients; these expansions are derived from observations of the spacecraft acceleration in the line-of-sight (LOS) to Earth. Either LOS observations or the derived spherical harmonic coefficients may be used to obtain the admittance [McKenzie and Nimmo, 1997; McKenzie et al., 2002].

[13] The need to attenuate short wavelength noise when calculating the spherical harmonic coefficients tends to reduce the resulting admittance at short wavelengths [McKenzie and Nimmo, 1997], so at short wavelengths LOS estimates are likely to be more reliable. Furthermore, it has been shown that the poorly determined transverse acceleration of the spacecraft can introduce errors into the derived spherical harmonic representation of the gravity [McKenzie et al., 2002], owing to the orbit geometry. For these reasons, this work uses LOS acceleration profiles rather than spherical harmonics. All admittance estimates suffer from a tradeoff between the area over which the estimate is made, and the uncertainty in the estimate [Simons et al., 1997].

[14] The raw LOS data (D-N. Yuan, personal communication, 2001) [see also McKenzie et al., 2002] consist of records of residual LOS velocity (relative to that calculated from a low-order gravity model) as a function of position and time. The records are generally spaced 20 s apart and the orbital velocity is about 3 km s<sup>-1</sup>. In order to obtain the full LOS acceleration, the residual velocity was added to that from the gravity model MGS75D [Yuan et al., 2001] and then a centered first difference taken to obtain the acceleration. Note that this gravity model has an a priori constraint applied above degree 59 [Yuan et al., 2001]

**Table 1.** Constants Adopted for Admittance Models

Quantity	Unit	Value
Young's modulus	Pa	$1.0 \times 10^{11}$
Poisson's ratio	—	0.25
$\rho_m$	Mg m <sup>-3</sup>	3.4
$\rho_l$	Mg m <sup>-3</sup>	3.0
$t_u$	km	3
$g$	m s <sup>-2</sup>	3.72

which may cause underestimates in the spherical harmonic (but not the LOS) admittance at higher degrees [McKenzie and Nimmo, 1997]. The predicted LOS acceleration based on an  $l = m = 180$  model of the observed topography was calculated using an assumed admittance of 1 mGal/km. The predicted acceleration included a correction for the finite nature of the topography [McGovern *et al.*, 2002; Wiczorek and Philips, 1998]. Prior to calculation of the LOS admittance, both data sets were interpolated onto profiles with a constant spacing of 60 km. Profiles consisting of fewer than 50 data points were not used. Further details of the LOS admittance technique are given by McKenzie and Nimmo [1997] and McKenzie *et al.* [2002].

[15] In order to find the best fit model to the data, the admittance given by equations (4)–(9) was calculated in the wavelength range 350–1800 km as a function of  $T_e$ ,  $t_c$ ,  $\rho_l$  and  $F$ . The upper limit on wavelength was chosen so that the effects of spherical geometry (not modeled here) were unlikely to be significant. The misfit  $H$  (as defined by McKenzie and Fairhead [1997]) between observations and theory was minimized by varying the four parameters in the ranges 1–200 km, 1–400 km, 2.0–3.0 Mg m<sup>-3</sup> and 0–5, respectively. Models which match the data without overfitting have  $H \sim 1$  [McKenzie, 2002]. In this work, misfits greater than 1.5 times the minimum misfit value  $H_{min}$  were assumed to be unacceptable. Parameters which were held constant are given in Table 1. The effect of uncertainties in the assumed values of  $\rho_l$ ,  $\rho_m$  and  $t_u$  are discussed in section 4.2.

#### 4. Results

[16] Figure 1a shows the LOS admittance estimates for an area of the dichotomy (110°E to 220°E, 40°S to 20°N). The admittance is close to zero at long wavelengths (>1000 km), increases over a relatively short wavelength range, and approaches a nearly constant value at short wavelengths (<500 km). Low values of  $Z$  at around 1000 km suggest that either  $t_c$  is small or that there is a significant fraction of (coherent) subsurface loading. However, the fact that  $Z$  does not become negative places an upper bound on  $F$ . The non-zero admittance at wavelengths >2000 km may be due to either convection [McKenzie, 1994] or the sphericity of the planet [Turcotte *et al.*, 1981], neither of which are modeled in this work.

[17] Figure 1b shows the coherence, which is high in the wavelength range over which the admittance increases and then decreases to  $\sim 0.1$  in the wavelength range 500–700 km. At wavelengths shorter than 400 km the coherence falls off rapidly, presumably because upwards attenuation reduces the LOS acceleration signal relative to the instrumental noise. The lack of coherence at long wavelengths is probably due to incoherent subsurface loading. Such loads are a natural result of erosion and sedimentation [McKenzie,

2002], and make it difficult to use the coherence to constrain the parameters of interest.

#### 4.1. Single-Layer Model

[18] The data in Figure 1 may be fit by a single-layer model ( $t_u = t_c$ ). The results of such a model are summarized in Table 2, and demonstrate that the uniform crustal density  $\rho_u$  required is 2.5 Mg m<sup>-3</sup>. As will be discussed in section 4.2, this density is significantly lower than the values  $\geq 3.0$  predicted from meteorites or measured in other admittance

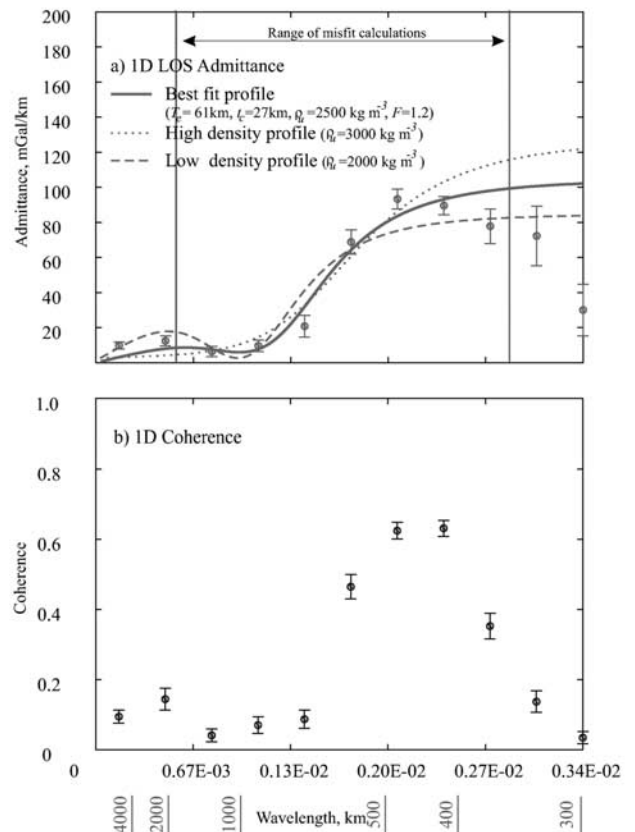


**Figure 1.** Mars admittance estimates from LOS data (1D) as a function of wavenumber. Horizontal axis is  $1/\text{wavelength}$ . Topography was assumed to be noise-free. Circles are data, calculated from LOS acceleration profiles over the area 40°S to 20°N, 100°E to 220°E, and expected acceleration based on  $l = m = 180$  spherical harmonic expansion of MOLA gridded topography incorporating a correction for finite amplitude topography. Solid line is minimum misfit theoretical admittance profile. This profile is for a two-layer crust (see text) with parameters given in Table 1. Dashed and dotted lines are minimum misfit theoretical profiles with densities fixed *a priori* at 2.0 and 3.0 Mg m<sup>-3</sup>, respectively. Vertical lines show wavelength range over which misfit  $H$  is calculated. The value of  $H$  for the dashed and dotted lines are 1.45 and 1.40 times the minimum  $H_{min}$ . b) One-dimensional coherence as a function of wavenumber for same area.

**Table 2.** Results of Misfit Minimization of LOS Admittance Data Shown in Figure 1a<sup>a</sup>

Quantity	Unit	Uniform Crust	Min. Misfit ( $\rho_u$ Fixed)	$\rho_u$ Fixed	$F$ Fixed
$\rho_u$	Mg m <sup>-3</sup>	2.5 <sub>(2.0–3.0)</sub>	2.5	3.0	2.9
$t_c$	km	29 <sub>(1–153)</sub>	27 <sub>(1–75)</sub>	3 <sub>(1–13)</sub>	1
$T_e$	km	59 <sub>(21–115)</sub>	61 <sub>(37–89)</sub>	27 <sub>(21–41)</sub>	23
$F$	–	1.2 <sub>(0–5)</sub>	1.2 <sub>(0.4–2.6)</sub>	0.2 <sub>(0–0.6)</sub>	0
Misfit	–	1.30	1.30	1.84	1.94

<sup>a</sup>“Uniform crust” is the minimum misfit solution for a uniform crust ( $\rho_u = \rho_u$ ) obtained by varying  $t_c$ ,  $T_e$ ,  $F$ , and  $\rho_u$  in the ranges 1–400 km, 1–200 km, 0–5 and 2–3 Mg m<sup>-3</sup>, respectively. “Min. Misfit” is minimum misfit two-layer solution obtained by the same method but with  $\rho_u$  fixed at the minimum misfit value. “ $\rho_u$  fixed” is the minimum misfit solution but with a different value for  $\rho_u$ . “ $F$  fixed” is the minimum misfit solution with  $F$  fixed at 0 and  $t_c$ ,  $T_e$  and  $\rho_u$  varying. Figures in parentheses give ranges of solutions for which the misfit  $H$  is less than 1.5 than the minimum misfit ( $H_{min} = 1.30$ ).

studies. Fixing the density at 3.0 Mg m<sup>-3</sup> results in a 40% increase in misfit; the misfit is particularly obvious at wavelengths  $\leq 500$  km. Equation 2 shows that the admittance at short wavelengths depends only on the value of  $\rho_u$ . The admittance over wavelengths 350–500 km is  $90 \pm 10$  mGals/km, which implies  $\rho_u = 2.14 \pm 0.24$ . This value is slightly smaller than the global minimization result because it assumes completely rigid support over the wavelength range used.

#### 4.2. Two-Layer Crust

[19] Since the single layer model predicts a bulk crustal density at odds with expectations, a two-layer model was used to fit the data with  $\rho_l$  and  $t_u$  fixed at 3.0 Mg m<sup>-3</sup> and 3 km, respectively. Figure 1a shows the global minimum misfit solution in this case (bold line) and two poorer fits ( $H \approx 1.5H_{min}$ ) obtained by fixing  $\rho_u$  at 2.0 Mg m<sup>-3</sup> (dashed line) and 3.0 (dotted line), respectively. The dashed line fits the (noisy) short wavelength data, but at the expense of poorer fits to the intermediate ( $\sim 500$  km) wavelength data. Table 2 summarizes the sets of parameters thus obtained for the minimum misfit case. These values are almost identical to those found for the single-layer case. However, the important difference is that the density structure of the crust is now more in line with expectations, since the model has a near-surface low density (2.5 Mg m<sup>-3</sup>) layer underlain by a denser layer.

##### 4.2.1. Uncertainties in Results

[20] Figure 1 shows that a 50% increase in misfit produces a noticeably poorer fit to the data. Because the density  $\rho_u$  is well-constrained by the short wavelength admittance (see above), it may be appropriate to take this value as known. For a fixed  $\rho_u$  of 2.5 Mg m<sup>-3</sup> and varying  $t_c$ ,  $T_e$  and  $F$  such that the misfit does not exceed  $1.5H_{min}$  results in ranges of 1–75 km, 37–89 km and 0.4–2.6, respectively. Relaxing the constraint on  $\rho_u$  results in increased ranges of 1–111 km, 21–113 km and 0–4, respectively. Estimates of the admittance using spherical harmonics (not shown) provide slightly smaller values at short wavelengths. Upper bounds on  $t_c$  and  $T_e$  for these estimates are 127 km and 89 km, respectively. However, as noted above, the spherical harmonic admittance estimates are likely to be less accurate than those derived directly from the LOS acceleration [McKenzie *et al.*, 2002].

[21] The relatively short wavelength range over which the admittance increases is characteristic of bottom loading.

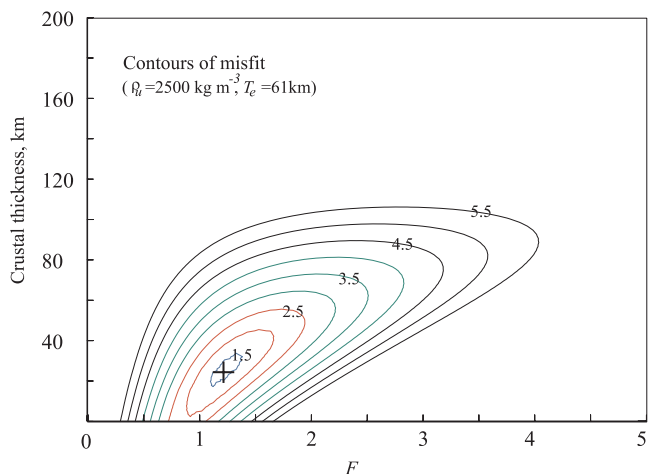


**Figure 2.** Contours of misfit  $H$  as a function of  $F$  and  $t_c$  assuming  $\rho_u = 2.5$  Mg m<sup>-3</sup> and  $T_e = 61$  km. Cross denotes minimum misfit point (see Table 2). Contour intervals are  $0.5H_{min}$ .

Fixing the fraction of bottom loading  $F$  to be 0 results in smaller best fit values of  $T_e$  and  $t_c$ , with a misfit 50% larger than the global minimum (see Table 2). Therefore, if it is assumed *a priori* that  $F = 0$ , the result may be an underestimate in  $T_e$  and  $t_c$  and an overestimate in  $\rho_u$ . The tradeoff between  $F$  and  $t_c$  is shown in Figure 2 for fixed  $\rho_u$  and  $T_e$ , demonstrating that lower values of  $F$  produce lower values of  $t_c$ .

[22] As noted above,  $\rho_u$  is best constrained by the short wavelength admittance. Fixing  $\rho_u$  at the expected bulk crustal density of 3.0 results in a 40% increase in misfit, and a reduction in  $T_e$ ,  $t_c$  and  $F$  (see Table 2). For a fixed density, there is a tradeoff between  $T_e$  and  $t_c$  [Barnett *et al.*, 2000]. Figure 3 plots contours of misfit as a function of  $T_e$  and  $t_c$  and shows the inverse nature of the relationship.

##### 4.2.2. Uncertainties in Fixed Parameters

[23] In the preceding discussion it was assumed that the parameters in Table 1 are well known, which is not the case

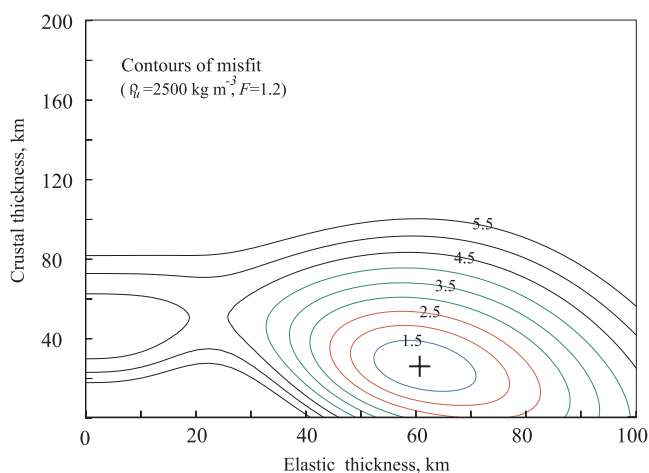


**Figure 3.** Contours of misfit  $H$  as a function of  $T_e$  and  $t_c$  assuming  $\rho_u = 2.5$  Mg m<sup>-3</sup> and  $F = 1.2$ . Cross denotes minimum misfit point (see Table 2). Contour intervals are  $0.5H_{min}$ .

for  $\rho_l$ ,  $t_u$  and  $\rho_m$ . It therefore remains to be seen whether varying these quantities significantly affects the results.

[24] The surface density  $\rho_u = 2.5 \text{ Mg m}^{-3}$  from the results above, but the crustal density at depth  $\rho_l$  is unknown. Perhaps the most reliable determination comes from the short wavelength LOS estimates of *McKenzie et al.* [2002], who found the surface density at Tharsis and Elysium to be about  $3.0 \text{ Mg m}^{-3}$ . *Turcotte et al.* [2002] obtained an essentially identical value. Since the surface lavas are relatively recent [*Hartmann et al.*, 1999] and thus unlikely to be seriously affected by impact brecciation, this value is probably a good estimate of the density of unfractured crust. Although samples of Martian meteorites have densities around  $3.25\text{--}3.30 \text{ Mg m}^{-3}$  [*Consolmagno and Britt* 1998; *Lodders*, 1998] they are typically cumulates [*McSween*, 1994], and are thus not easy to relate to bulk crustal compositions.

[25] Changes in  $\rho_l$  affect  $Z_1$  and  $Z_2$  in opposite directions (equations 5 and 6), and thus the net effect on  $Z$  is small. Recalculating the minimum misfit solution with  $\rho_l$  varying between  $2.9 \text{ Mg m}^{-3}$  and  $3.1 \text{ Mg m}^{-3}$  causes no difference to the results. Similarly, varying  $\rho_m$  between  $3.3 \text{ Mg m}^{-3}$  and  $3.5 \text{ Mg m}^{-3}$  causes less than a 5% change in the results.

[26] The value of  $t_u$  is also uncertain. By analogy with seismic results from the Moon, *Clifford* [1993] estimated that the decay length of crustal porosity for Mars was  $\sim 3$  km. On the Moon, the crust is thought to be essentially intact at depths greater than  $\sim 20$  km [*Simmons et al.*, 1973]; the same is presumably true at about half this depth on Mars, due to the greater gravity. As with  $\rho_l$ , equations (5) and (6) indicate that changes in  $t_u$  will have little net effect on the value of  $Z$ . Recalculating the minimum misfit solution with  $t_u$  varying in the range 1–20 km changed the minimum misfit values of  $t_c$  and  $T_e$  by less than 10%.

[27] One factor which has been ignored is the possibility of preexisting topography along the upper-lower crust interface. Since the density contrast between upper and lower crust is probably similar to that between lower crust and mantle, neglect of such loads is a weakness of the model. However, incorporating them would introduce further uncertainties into an already weakly constrained problem. Since the tectonic and elevation differences between the northern and southern hemispheres strongly suggest that there was preexisting Moho topography, it was considered more important to include this latter effect.

[28] The admittance equations (4)–(10) take no account of the sphericity of the planet, and for this reason wavelengths  $>1800$  km are not included in the misfit calculations. Using a single layer model, the effect of incorporating sphericity causes no change in the value of  $T_e$ , but an increase in  $t_c$  to 45 km offset by a corresponding increase in  $F$  to 1.6 (c.f. Table 2). These changes are considerably smaller than the estimated uncertainties in  $t_c$  and  $F$  and are therefore of secondary importance.

## 5. Discussion and Conclusions

[29] Equation 2 and the short wavelength admittance values demonstrate that the surface density of the crust is significantly less than the assumed density at depth of  $\sim 3.0 \text{ Mg m}^{-3}$  (section 4.1). A similar conclusion was reached by *McKenzie et al.* [2002]. Thus, a two-layer crustal model is required to fit the data. Furthermore, the results in Table 2

show that surface loading alone ( $F = 0$ ) provides an unsatisfactory fit to the observations (section 4.2). It therefore appears that the least complex model required by the observations is one of a two-layer crust with both subsurface and surface loading. The disadvantage of this conclusion is the consequent large number of variables.

[30] In this work only four of these variables  $-\rho_u$ ,  $t_c$ ,  $T_e$  and  $F$  are solved for. Varying the  $\rho_l$ ,  $\rho_m$  and the thickness of the upper crust  $t_u$  does not significantly affect the results (section 4.2). Assuming that a 50% increase over  $H_{min}$  is the maximum acceptable misfit, bounds can be placed on all four variables (Table 2). If the density  $\rho_u$  is considered to be well constrained, the acceptable range of the other parameters is reduced.

[31] Based on the fact that both Argyre and Hellas appear to be compensated, *Nimmo and Stevenson* [2001] argued that the minimum crustal thickness beneath the southern highlands is about 45 km for a mean crustal density  $\rho_c = 2.8\text{--}2.9$ ; *Zuber et al.* [2000] reached similar conclusions. Although these estimates may be affected by errors in the spherical harmonic gravity representation [*McKenzie et al.*, 2002], they are consistent with the mean crustal thickness range (1–75 km) estimated above. Note that the southern hemisphere crustal thickness may be up to 10 km greater than the mean value of  $t_c$  since the long wavelength topography variations are probably isostatically supported [*Zuber et al.*, 2000].

[32] Various other authors have investigated crustal and elastic thicknesses in the southern highlands. *Turcotte et al.* [2002] used a spherical harmonic representation of geoid and topography to find  $\rho_c = 2.96 \pm 0.5 \text{ Mg m}^{-3}$  and  $t_c = 90 \pm 10$  km for the Hellas basin. *Yuan et al.* [2001] used a similar technique to obtain a global mean reference crustal thickness of 100 km. These estimates are roughly consistent with the upper bound on  $t_c$  derived here.

[33] *Zuber et al.* [2000], *McGovern et al.* [2002], and *McKenzie et al.* [2002] found values of  $T_e$  for the southern highlands of 0–20 km, 0–20 km and 15 km, respectively. There are two likely reasons for the larger value of  $T_e$  found in this work compared with the other results. One is that, since about half of the area studied is in the more rigid northern plains, the value found may represent an average of two different elastic thicknesses [*Forsyth*, 1985]. Second, there is a tradeoff between  $T_e$  and the value of subsurface loading assumed (see section 4.2). The  $F - T_e$  tradeoff may be illustrated by the south pole results of *McKenzie et al.* [2002]. The minimum misfit solution to these is  $t_c = 21$  km,  $T_e = 11$  km and  $\rho_u = 2.9 \text{ Mg m}^{-3}$  if  $F$  is fixed to 0. However, relaxing this constraint reduces the misfit from 2.91 to 0.97 and increases  $t_c$ ,  $T_e$  and  $F$  to 43 km, 51 km and 1.8, respectively, while  $\rho_u$  is reduced to  $2.1 \text{ Mg m}^{-3}$ . Thus, if the degree of bottom loading is underestimated, the values of both  $T_e$  and  $t_c$  are likely to be underestimates. This is a potentially important result, since elastic thickness estimates are often used to constrain geothermal gradients and thus thermal histories.

[34] The discrepancy with the *McGovern et al.* [2002] results is more surprising, since these authors find evidence for variable amounts of subsurface loading in the southern highlands. The most likely explanation is that the  $T_e$  estimate in this work is biased to a higher value by the northern plains.

[35] On Earth, the thickness of the elastic layer is thought to be controlled by the depth to an isotherm around 450–

600°C [Watts and Daly, 1981]. Thus, if the minimum misfit  $T_e$  values obtained here of 50–60 km is applicable to the southern highlands, the implied heat flux is 25–40 mW m<sup>-2</sup>. Mantle heat fluxes on Mars at 4 Gyr b.p. were probably 50–60 mW m<sup>-2</sup> [Nimmo and Stevenson, 2001], assuming radiogenic element concentrations similar to terrestrial ones. One possible resolution of this apparent disagreement is that early crustal differentiation concentrated radiogenic elements into the crust, reducing the thermal gradient at depth [McLennan, 2001].

[36] The admittance estimates in this work assume that the main source of noise is gravity anomalies which are incoherent with the topography [McKenzie and Fairhead, 1997]. Plots of the spherical harmonic gravity and topography [Smith et al., 1999a, 1999b] and the behaviour of the long-wavelength coherence (Figure 1b) suggests that  $Z$  as defined in equation (1) is the appropriate estimate to use. However, errors in the topography, or a variation in  $T_e$  over the area considered may result in a reduction in  $Z$  [Forsyth, 1985]. If  $Z$  is an underestimate of the true admittance, then so are the values of  $t_c$  and  $T_e$  in Figure 3.

[37] There are three important conclusions from section 4. First, the surface density of the area modeled is lower than that expected for the bulk of the Martian crust, suggesting that a two-layer crustal model is appropriate. Second, pure surface loading ( $F = 0$ ) does a poor job of fitting the data, suggesting that subsurface loading is important, and that methods assuming that  $F = 0$  may underestimate  $t_c$  and  $T_e$ . Finally, the likely value of  $t_c$  over the area of interest is in the range 1–75 km with a minimum misfit value of 27 km. The assumption that Hellas and Argyre are Airy compensated provides a lower bound on the southern highland crustal thickness of 45 km. In the area of the dichotomy studied, therefore, the likely mean Martian crustal thickness is  $55 \pm 20$  km. Previously, both Zuber et al. [2000] and Nimmo and Stevenson [2001] argued that because the dichotomy has not decayed over 4 Gyr, the crustal thickness must be less than  $\sim 100$  km. Hence, the bound derived here is compatible with, and provides a slightly better constraint than, these previous estimates.

[38] **Acknowledgments.** The author thanks Magdalene College, Cambridge, the NASA Mars Data Analysis Program, and the Royal Society for supporting this work. The help of Dah-Ning Yuan and Dan McKenzie is gratefully acknowledged. Don Turcotte and an anonymous reviewer greatly improved this manuscript.

## References

Barnett, D., F. Nimmo, and D. McKenzie, Elastic thickness estimates for Venus using line of sight accelerations from Magellan cycle 5, *Icarus*, 146, 404–419, 2000.

- Clifford, S. M., A model for the hydrologic and climatic behavior of water on Mars, *J. Geophys. Res.*, 98, 10,973–11,016, 1993.
- Consolmagno, G. J., and D. T. Britt, The density and porosity of meteorites from the Vatican collection, *Meteoritics*, 33, 1231–1241, 1998.
- Esposito, P. B., et al., Gravity and topography, in *Mars*, edited by H. H. Kieffer et al., pp. 209–248, Univ. of Ariz. Press, Tucson, 1992.
- Forsyth, D. W., Subsurface loading and estimates of flexural rigidity of continental lithosphere, *J. Geophys. Res.*, 90, 12,623–12,632, 1985.
- Hartmann, W. K., et al., Evidence for recent volcanism on Mars from crater counts, *Nature*, 397, 584–586, 1999.
- Lodders, K., A survey of shergottite, nakhlite and chassigny meteorites whole-rock compositions, *Meteoritics*, 33, A183–A190, 1998.
- McGovern, P. J., S. C. Solomon, D. E. Smith, M. T. Zuber, M. Simons, M. Wiczeorek, R. J. Phillips, G. A. Neumann, O. Aharonson, and J. W. Head III, Localized gravity/topography admittance and correlation spectra on Mars: Implications for regional and global evolution, *J. Geophys. Res.*, 107, doi:10.1029/2002JE001854, in press, 2002.
- McKenzie, D., The relationship between gravity and topography on Earth and Venus, *Icarus*, 112, 55–88, 1994.
- McKenzie, D., Estimating  $T_e$  in the presence of internal loads, *Earth Planet. Sci. Lett.*, in press, 2002.
- McKenzie, D., and D. Fairhead, Estimates of the effective elastic thickness of the continental lithosphere from Bouguer and free air gravity anomalies, *J. Geophys. Res.*, 102, 27,523–27,552, 1997.
- McKenzie, D., and F. Nimmo, Elastic thickness estimates for Venus from line of sight accelerations, *Icarus*, 130, 198–216, 1997.
- McKenzie, D., D. Barnett, and D.-N. Yuan, The relationship between Martian gravity and topography, *Earth Planet. Sci. Lett.*, 5, 1–16, 2002.
- McLennan, S. M., Crustal heat production and the thermal evolution of Mars, *Geophys. Res. Lett.*, 28, 4109–4122, 2001.
- McSween, H. Y., What we have learned about Mars from SNC meteorites, *Meteoritics*, 29, 757–779, 1994.
- Nimmo, F., and D. Stevenson, Estimates of Martian crustal thickness from viscous relaxation of topography, *J. Geophys. Res.*, 106, 5085–5098, 2001.
- Simmons, G., T. Todd, and H. Wang, The 25-km discontinuity and implications for lunar history, *Science*, 182, 158–161, 1973.
- Simons, M., S. C. Solomon, and B. H. Hager, Localization of gravity and topography: Constraints on the tectonics and mantle dynamics of Venus, *Geophys. J. Int.*, 131, 24–44, 1997.
- Smith, D. E., et al., The global topography of Mars and implications for surface evolution, *Science*, 284, 1495–1503, 1999a.
- Smith, D. E., et al., The gravity field of Mars: Results from Mars Global Surveyor, *Science*, 286, 94–97, 1999b.
- Turcotte, D. L., R. J. Willeman, W. F. Haxby, and J. Norberry, Role of membrane stresses in the support of planetary topography, *J. Geophys. Res.*, 86, 3951–3959, 1981.
- Turcotte, D. L., R. Shcherbakov, B. D. Malamud, and A. B. Kucinskas, Is the Martian crust also the Martian elastic lithosphere?, *J. Geophys. Res.*, 107(E11), 5091, doi:10.1029/2001JE001594, 2002.
- Watts, A. B., and S. F. Daly, Long wavelength gravity and topography anomalies, *Annu. Rev. Earth Planet. Sci.*, 9, 415–458, 1981.
- Wiczeorek, M. A., and R. J. Phillips, Potential anomalies on a sphere: Applications to the thickness of the lunar crust, *J. Geophys. Res.*, 103, 1715–1724, 1998.
- Yuan, D.-N., W. L. Sjogren, A. S. Konopliv, and A. B. Kucinskas, The gravity field of Mars: A 75th degree and order model, *J. Geophys. Res.*, 106, 23,377–23,401, 2001.
- Zuber, M. T., et al., Internal structure and early thermal evolution of Mars from Mars Global Surveyor topography and gravity, *Science*, 287, 1788–1793, 2000.

F. Nimmo, Department of Geological Sciences, University College London, Gower Street, London WC1E 6BT, England, UK. (nimmo@gps.caltech.edu)